University of Bath

Alternative formats
If you require this document in an alternative format, please contact:
openaccess@bath.ac.uk

Journal Pre-proof

Dissecting the stability of Atezolizumab with renewable amino acid-based ionic liquids: Colloidal stability and anticancer activity under thermal stress

Bayan Alkhawaja, Faisal Al-Akayleh, Zaid Al-Rubaye, Ghayda'a Al-Dabet, Muna Bustami, Maisa'a Smairat, Ahmed S.A.A. Agha, Jehad Nassereden, Nidal Qinna, Andreas Michael, Andrew G. Watts

This is a PDF file of an article that has undergone enhancements after acceptance, such as the addition of a cover page and metadata, and formatting for readability, but it is not yet the definitive version of record. This version will undergo additional copyediting, typesetting and review before it is published in its final form, but we are providing this version to give early visibility of the article. Please note that, during the production process, errors may be discovered which could affect the content, and all legal disclaimers that apply to the journal pertain.

1

Dissecting the stability of Atezolizumab with renewable amino acid-based ionic liquids: Colloidal stability and anticancer activity under thermal stress

Bayan Alkhawaja[1*], Faisal Al-Akayleh[1*], Zaid Al-Rubaye[1], Ghayda'a Al-Dabet[2], Muna Bustami[1], Maisa'a Smairat[1], Ahmed S.A.A Agha[1], Jehad Nassereden[3], Nidal Qinna[2], Andreas Michael[4,] Andrew G Watts[4]

[1] Faculty of Pharmacy and Medical Sciences, University of Petra, Amman 11196, Jordan
[2] University of Petra Pharmaceutical Center, Faculty of Pharmacy and Medical Sciences, Petra University, Amman 11196, Jordan
[3] Department of Pharmaceutical Sciences, Faculty of Pharmacy, Zarqa University, Zarqa 13110, Jordan
[4] Department of Life Sciences, University of Bath, Claverton Down, BA2 7AY, Bath, UK

*Corresponding authors' email:

bayan.alkhawaja@uop.edu.jo, University of Petra, Amman 11196, Jordan

falakayleh@uop.edu.jo, University of Petra, Amman 11196, Jordan

Abstract

Monoclonal antibodies (mAbs) have revolutionised the biopharmaceutical market. Being proteinaceous, mAbs are prone to chemical and physical instabilities. Various approaches were attempted to stabilise proteins against degradation factors. Ionic liquids (ILs) and deep eutectic solvents (DESs) have been established as green solvents for ever-increasing pharmaceutical and biopharmaceutical applications. Hence, amino acid (AA)-based ILs, were used for the first time, for mAb stabilization. Choline (Ch)-based DESs were also utilised for comparison purposes. The prepared ILs and DESs were utilised to stabilise Atezolizumab (Amab, anti-PDL-1 mAb). The formulations of Amab in ILs and DESs were incubated at room temperature, 45 or 55 °C. Following this, the structural stability of Amab was appraised. Interestingly, Ch-Valine retained favourable structural stability of Amab with minimal detected aggregation or degradation as confirmed by UV-visible spectroscopy and protein Mass Spectroscopy. The measured hydrodynamic diameter of Amab in Ch-Valine ranged from 10.40 to 11.65 nm. More interestingly, the anticancer activity of Amab was evaluated, and Ch-Valine was found to be optimum in retaining the activity of Amab when compared to other formulations, including the control Amab sample. Collectively, this study has spotlighted the advantages of adopting the Ch-AA ILs for the structural and functional stabilising of mAbs.

Keywords: Ionic liquids, Deep eutectic solvents, Biocompatible and renewable ILs, Amino acid-based ILs, Stability of monoclonal antibodies, Atezolizumab.

Introduction

Deep eutectic solvents (DESs) and ionic liquids (ILs) have established themselves as cardinal and green solvents for ever-increasing industrial applications [1,2]. Owing to their intriguing stability, versatility and adaptability, the pharmaceutical implications of DESs and ILs have increased in the last two decades [3]. As such, DESs and ILs have been widely exploited in the drug delivery field of small molecules, such as transdermal and topical delivery of small hydrophobic drugs and molecules [4–6].

More interestingly, utilising DESs and ILs has gained ground in delivering, solubilising, stabilising and modifying biological drugs and enzymes [7–10]. Banerjee et al. described the use ILs as drug delivery systems of peptides and proteins, such as oral insulin delivery [11]. Moreover, employing ILs for stabilising proteins and enzymes and performing biocatalytic reactions, particularly for poorly soluble substrates, has also gained attention [12–14]. Extraction and purification of antibodies using bio-based ILs were described by Mondal et al. [15]. Interestingly, in the pursuit of achieving conjugation reactions in non-aqueous media, El-Shaffey and coworkers have utilised pyrrolidinium-based IL to perform protein conjugation reactions at 50 °C [16].

There has been a dearth of efforts to introduce the so-called environmentally-friendly, renewable and biodegradable ILs, including choline (Ch)-based ILs (Ch-ILs) and amino acid (AA)-based ILs, also known as the 3rd generation ILs [12,17]. Choline, an essential nutrient, is known to be non-toxic and biodegradable. Choline-based ILs are considered safe surrogates for other ILs counterparts [18,19]. With the potential of increasing their safety and biodegradability, Ch-ILs were prepared with AA to construct Ch-AA ILs. Ch-AA ILs are versatile tools in many pharmaceutical and biomedical fields. The different anions (AA) and their distinctive chemical and structural variabilities offer various tailoring possibilities for ubiquitous solubilisation, stabilisation, delivery and storage purposes [20–22].

Monoclonal antibodies (mAbs) have become crucial to cancer therapy and various inflammatory diseases [23]. They are known for their intriguing ability to target tumour cells and induce long-lasting anti-tumour effects [23]. As of 2021, more than 100 mAbs were granted approval for numerous indications [24]. Antibodies are large glycoproteins with a distinctive Y-shaped structure, and the therapeutic features of mAb are mainly related to its structure. Structurally, mAbs consist of two heavy and two light chains. Functionally, mAbs have two main fragments: the fragment antigen-binding (Fab) and the fragment crystallisable (Fc) region [25]. Using mAbs to fight against tumours has shifted towards targeting immune cells, also known as immune checkpoint inhibitors (ICIs). ICIs are mAbs that re-activate T cells to attack cancer by inhibiting physiological brakes. Anti-PD1 or anti-PDL-1 antibodies are among the most commonly used ICIs [26–30]. In this work, Atezolizumab (Amab), an anti-PDL-1

antibody, was selected as a model therapeutic mAb to perform stability and activity studies using various Ch-AA ILs.

Although mAbs and their related products are among the fastest growing class of biologics [31], long-term storage and stability of biological drugs have hindered their widespread pharmaceutical implications [32]. The physical and chemical stability of the biotherapeutic molecule is of utmost importance as it affects the safety and efficacy of the product. [33,34]. Using the appropriate solvents and excipients are cardinal to maintain the structural and colloidal stability of antibodies as well as they play major impact in reducing their toxicity potential [35]. To this end, several biocompatible approaches and solvents were utilised to enhance the stability of antibodies. Dhiman and coworkers demonstrated the positive impact of Ch-based DESs on the stability of immunoglobulin G (IgG) antibody [36]. Moreover, Ch-chloride IL was utilised to stabilise and store IgG4 antibody up to one year at 4 °C [37]. Similarly, IgG4 antibodies stabilised and reduced aggregation propensity were achieved using Ch-based IL in their formulation [38]. Altogether, there are no clear answers to whether using ILs or DESs would be more appropriate in antibody formulations. In addition to the lack of activity evaluation of the studied antibodies, most of them were non-therapeutic models.

Thus, we tend to compare the use of DESs with ILs as green solvents for stabilising and retaining the activity of therapeutic mAbs, notably against thermal stress. Although there have been significant advancements and an understanding of protein-IL interactions, a gap remains, and further exploration is required. Mainly, limited work focuses on exploring and comparing various Ch-AA ILs potential to stabilise therapeutic mAbs. Therefore, our research discloses, for the first time, the impact of employing biocompatible Ch-AA ILs on mAb's structural and colloidal stability and, more importantly, its biological activity. This work also studied examples of commonly used DESs for comparison purposes.

Materials and Methods

Choline chloride (ChCl) malonic acid (Mal) and 1-Butyl-1-methylpyrrolidinium trifluoromethanesulfonate (BMPy) were obtained from Tokyo Chemical Industry Co., Ltd (TCI, Japan). L-amino acids were purchased from Sigma-Aldrich Chemical Company (USA). HPLC-grade ethanol (EtOH) was purchased from VWR (USA). Potassium Hydroxide (KOH) pellets were purchased from ScharLab (Spain). Urea was purchased from Chem-Lab (Belgium). Atezolizumab (Tecentriq) was kindly provided as a gift from Pharmaxo Scientific. A pre-stained ladder (PageRuler™) was obtained from ThermoFisher. Trypsin/EDTA was purchased from Biowest®

(USA). Phosphate-buffered saline (PBS) was obtained from EuroClone® (Netherlands). DMSO was purchased from Fischer Chemicals (China), and MTT was obtained from PhytoTech Labs (USA).

Preparation of ChCl-based DESs

The binary mixture of ChCl and Mal was prepared by mixing ChCl (hydrogen bond donor) and Mal (hydrogen bond acceptor) according to the previously described procedure (Figure 1A) [39]. ChCl and Mal were mixed in an equimolar ratio and kept stirring at room temperature until a clear and homogenous liquid was obtained [39,40]. To prepare ChCl-Urea DES, ChCl and Urea were mixed in a ratio of 1:2. The mixture was stirred at 80 °C until a clear and homogeneous liquid was achieved [41]. The attained DESs were used directly without any further purification.

Preparation of Ch-AA ILs

The binary mixtures of Ch-AA were prepared by mixing ChCl and each amino acid in a 1:1 molar ratio according to the previously described procedure [42] (Figure 1B). Each AA was mixed with excess potassium hydroxide (KOH) in ethanol (EtOH). Subsequently, ChCl was added to the AA suspension. The mixture was stirred at room temperature (RT) for 4 hrs. Due to the solubility limitations of Choline-Aspartate Ch-Asp, the mixture was heated up to 80 °C to attain the IL. Then, the formed KCl precipitate was filtered off, and water and EtOH were removed under reduced pressure. The resulting ILs were dried using a vacuum oven for 24 h at 70 °C.
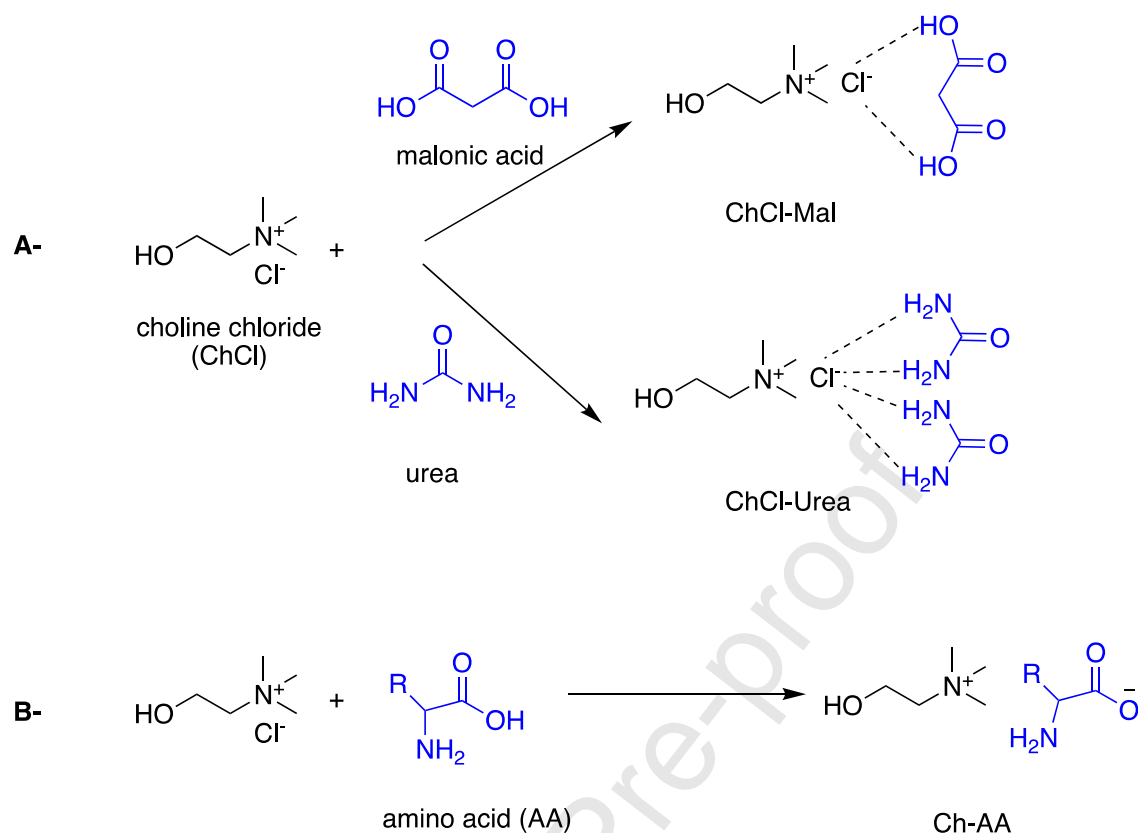
Figure 1. Preparation of choline-based mixtures. A) Preparation of ChCl-based DESs. B) Preparation of Ch-AA ILs.

Characterisation of Ch-based DESs and ILs

Nuclear Magnetic Resonance (NMR)

NMR datasets were collected on a 500-MHz Bruker instrument using DMSO-d_6 (Figure S1-8). Data is reported for ^{1}H: chemical shift (δ) in ppm (multiplicity, J coupling constant in Hz, number of protons); and for ^{13}C: chemical shift in ppm. Multiplicity is presented as follows: s (singlet), d (doublet), t (triplet), q (quartet), m (multiplet), dd (doublet of doublet), dt (doublet of triplets), td (triplet of doublet). NMR assignments are outlined in the supplementary file.

Rheology Study

To investigate the rheological properties of the DESs and ILs, a rotational rheometer (Physica MCR 302, Anton Paar) was used. The rotational rheometer was equipped with a parallel plate geometry to accurately measure the rheological properties of the liquids. Experiments were

6

conducted at 25°C to obtain precise shear rate and stress readings data. Torque values were calculated based on the resistance presented by each mixture when subjected to a set rotational speed. In addition, the shear strain could be deduced from torque measurements combined with known parameters of the device setup. The rheometer was calibrated beforehand. Rheological tests were analysed using computer-controlled rheocompass software (Anton Paar).

pH

The pH of the prepared ILs and DESs was measured using a Jenway 3510 pH meter. Dilutions at 10%, 20% and 40% w/w% of each ILs and DESs were prepared in deionised water.

Preparation of Amab formulations in Ch-based DESs and ILs

Amab concentration was calculated by measuring the absorbance at 280 nm using a plate reader (Thermo Scientific Multiskan™ Sky, USA) at room temperature (RT). Amab was buffer exchanged into deionised water using an Ultra centrifugal filter (10k MWCO). Formulation of DESs or ILs of Amab was prepared as follows: To DESs or ILs (0.80 g), an aqueous solution of Amab (25 mg/ml, 0.20 g in deionized water) was added. The final concentration of H_2O was kept equal to or lower than 25 w% to keep the solution in the (water-in-IL) category. In water-in-IL form, the structure of the ILs is the cardinal factor governing the properties of the solution, and the desirable features of ILs are maintained [20].

UV-visible spectroscopy

UV-visible spectroscopy (245-600 nm) was measured directly in the same IL or DES formulation using a plate reader (Thermo Scientific Multiskan™ Sky, USA). The aggregation of Amab samples were evaluated using an aggregation index (AI) value. AI values were calculated using 280 and 340 nm values using the following equation;

$$AI = {A340}/{(A280 - A340)} * 100$$

Measuring hydrodynamic diameter using dynamic light scattering (DLS)

The aggregation behaviour of the protein with ILs and DESs has been characterised using DLS. Measurements were performed using a Zetasizer Nano Series ZS (Malvern Instruments, UK) apparatus equipped with a 633 nm laser. A non-invasive back-scattering technique (173º) was used for detection. 25 μL of each sample were further diluted with deionised water to a concentration of 0.25 mg/ml. Five measurements (each with 20 runs) were performed for particle size determination. All the samples were allowed to equilibrate for 30 minutes at 25 ºC. The hydrodynamic diameter (D_r) and Polydispersity Index (Pdi) were reported. The device used a cumulants analysis to give a z-average diffusion coefficient and a width parameter known as the Pdi. The diffusion coefficient (D) is converted to a size (hydrodynamic diameter (D_r)) using the dispersant viscosity and some instrumental constants according to the Stokes-Einstein equation [43]. Herein, some of the Pdi values were above 0.5 due to the polydispersity and aggregation potential.

Sodium dodecyl sulphate polyacrylamide gel electrophoresis (SDS-PAGE)

SDS-PAGE (Invitrogen™ Mini Gel system) was employed to resolve protein samples. Precast Bis-Tris, 10-well protein gels (10%) were utilised and run using MES-SDS running buffer (NuPAGE™). Protein samples were buffer exchanged into deionised water. Samples were made to 2 mg/mL where possible. The protein samples were mixed with either reducing or non-reducing loading dye in a 1:1 ratio and heated at 75 °C for 3 minutes. The size of the proteins (Mwt) was estimated using a pre-stained ladder (PageRuler™, ThermoFisher).

Protein Mass spectroscopy (MS)

Protein samples were buffer exchanged into deionised water. Samples were made to 1 mg/mL where possible. LC-MS analysis was performed using an Agilent Electrospray Quadrupole Time-of-Flight (ESIQTOF) 6545. The MS was operated in positive ionisation mode. The Data was analysed using MassHunter Quantitative Analysis B0.07.

The biological activity of Amab in the presence of Ch-based DESs and ILs (MTT assay)

After assuring that the EMT6 cells were in the log phase, and the confluency was approximately 80%, cells were harvested from culture flasks by enzymatic digestion (trypsin/EDTA) (Biowest®,

USA). 96-well plates were plated with $1x10^5$ cells/well and incubated for 24 hr in a 37°C humidified CO_2 incubator. Then, the medium was removed, and wells were washed once with 100 µl phosphate-buffered saline (PBS, EuroClone®, Netherlands). Following this, cells were treated with 100 µl of the Amab control (2, 10, 20, 40, 80, 100, 160, and 200 µg/ml). DMSO (25%) (Fischer Chemicals, China) was used as a positive control, and medium alone was used as a negative control. The plates were incubated for 24, 48 or 72 hrs in a 37 °C humidified CO_2 incubator. Finally, cell morphology was evaluated using an inverted microscope (ZEISS, GmbH), 40 µl of the culture medium was removed, and 50 µl of sterile MTT (PhytoTech Labs, USA) solution at a concentration of 2 mg/ml was added to each well and allowed to incubate for 3 hrs at 37 °C humidified CO_2 incubator. 100 µl of isopropanol was added to each well and shaken at room temperature to stop the reaction. The assay was quantified at 570 nm using a plate reader (Thermo Scientific Multiskan™ Sky, USA). Next, to confirm the stability of Amab in the DESs and ILs following their exposure to 55 °C, the MTT assay was repeated after determining the ideal incubation time described above.

Results and discussion

Selection, preparation and characterisation of DESs and ILs

The selection of the amino acids was based on their functional group (R group) as shown in Figure 1. Consequently, amino acids with aliphatic (Gly, Val, Pro), aromatic (Trp), acidic (Asp) and basic functional groups (Lys) were included in this work. For comparison purposes, commonly used DESs, including ChCl-Mal and ChCl-Urea [39,40] and BMPy [44] were prepared and studied in this work. The AA ILs and DESs and their characteristics are summarised in Table 1.
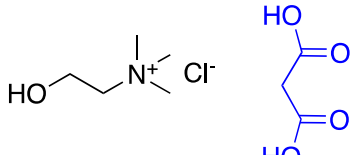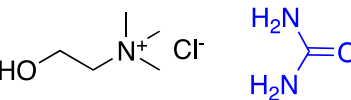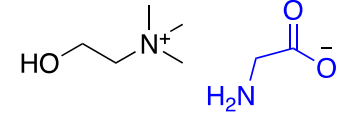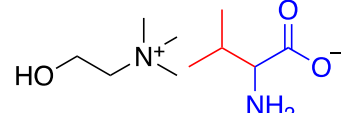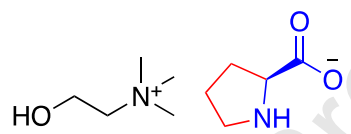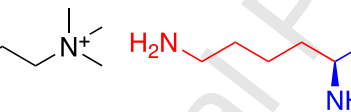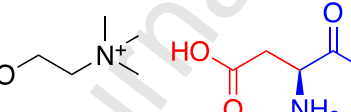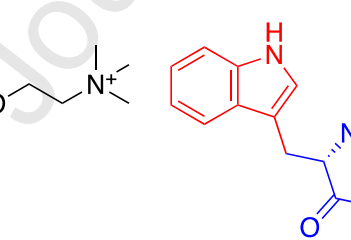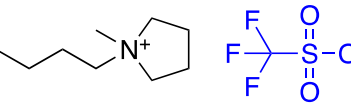
ChCl-based DESs were prepared using a simple procedure; the prepared DESs, namely ChCl-Mal and ChCl-Urea, were used without further purification, as described previously [39] .

The commonly procedures outlined in the literature for the preparation of AA ILs utilise choline hydroxide, which is corrosive, toxic and expensive. This counteracts the advantage of using bio-derived AAs in preparing bio-compatible AA ILs. In this study, Ch-AA ILs were prepared via acid-base reaction as described by Latini and coworkers [42]. Latini and his group have developed a

greener and more efficient method for preparing AA ILs based on the ionic metathesis between choline chloride, a non-toxic, cheap and easy-to-handle material, and potassium amino acid salts [42]. All the prepared Ch-AA ILs were characterised using ^{1}H and ^{13}C NMR prepared in deuterated DMSO. The spectrum and integration confirmed their stoichiometry (1:1 molar ratio with choline), except for Ch-Asp, which was found in a 2:1 ratio (Ch: Asp). It has been reported that AAs with carboxylic acid groups, including Asp, form solid ILs with choline at RT [45]. In our hands, we attained a liquid form of Ch-Asp, which could be attributed to the attained 2:1 ratio with choline ([Ch]$_2$-Asp). Ch-Asp will refer to ([Ch]2-Asp) in this study.

Table 1. The prepared and tested DESs and ILs in this work and their pH and viscosity.

Entry	Name	Structure	pH*	Viscosity (mPa·s)

			10%	20%	40%	**
1	ChCl-Mal		1.95	1.93	1.89	475.21
2	ChCl-Urea		7.14	7.52	7.97	577.39
3	Ch-Gly		11.25	11.37	11.88	161.36
4	Ch-Val		11.22	11.54	11.98	372 [46]
5	Ch-Pro		11.81	11.96	12.31	350.63
6	Ch-Lys		11.98	12.12	12.23	411.51
7	Ch-Asp		6.10	6.31	6.94	124.49*** 2060 [46]
8	Ch-Trp		10.23	11.10	11.27	1299.75
9	BMPy		4.47	4.34	4.29	77.92

*pH was measured after dilution of DES and IL at 10, 20 and 40 w/w% in deionized water.

**Averaged viscosity under shear rates from 1.6-100 1/s.

***for the dianionic mixture([Ch]$_2$-Asp)

Rheology Study of the DESs and ILs

Viscosity, which quantifies a fluid's resistance to flow, plays a crucial role in determining the effectiveness of DESs and ILs in pharmaceutical applications [47]. Therefore, significant efforts have been made to develop ILs with lower viscosity [48]. Table 1 displays that the DESs and ILs prepared in this study have a broad range of viscosities, ranging from 124.5 to 1300 mPa·s at 25 °C. The calculated viscosity values revealed the high viscosity of most prepared DESs and ILs and exhibited a pattern similar to the previously reported values [20]. The viscosity of the media plays a crucial role in the dissolution of proteins, including mAbs, and might impact its stability and propensity to aggregate [49,50]. However, the ideal viscosity for biomolecule colloidal stabilisation and preventing the aggregation or precipitation tendency can vary depending on numerous parameters, including the specific biomolecule of interest and the applications.

The intricacies of molecular interactions at the intersection of molecular weights and functional groups reveal the basis of the rheological behaviour of each Ch-AA IL. Regarding the highest calculated viscosity of Ch-Trp, the indole functional group (Table 1) allows for pi-pi interactions [51]. In addition, the Trp anion's considerable size eventually resulted in the highest viscosity among the tested ILs, and our results are comparable with the previously described behaviour of Ch-Trp [18]. On the other hand, Ch-Gly, with the anion being the simplest amino acid, has displayed low viscosity (161 mPa·s). With the AA size, a higher viscosity was observed with Ch-Val, Ch-Pro and Ch-Lys ILs, which might be ascribed to stronger van der Waals and hydrogen bond interactions. Val anion's aliphatic isopropyl group of Ch-Val produces stronger van der Waals forces due to the presence of isopropyl groups exhibiting higher viscosity than Ch-Gly [52]. The amine group's presence has increased the Ch-Lys viscosity (411.5 mPa.s), likely related to formed hydrogen bonds and electrostatic interactions [53]. Lastly, AA with carboxylic acids tends to have high viscosity [18] and is reported to be solid at RT[45]; here, the low attained viscosity of Ch-Asp could be attributed to the attained dianionic salt, as outlined earlier.

Regarding the DESs prepared in this work, namely ChCl-Urea and ChCl-Mal, both exhibited relatively intermediate viscosities. Ch-Urea IL contains two amine groups and one carbonyl, enabling the formation of a strong hydrogen bond network and explaining the relatively high viscosity achieved [54]. In contrast, the ChCl-Mal mixture has two carboxylic acid groups with strong hydrogen bond potential, explaining its relatively high viscosity [55].

The rheological behaviour of multi-component solvent-solute systems typically manifests as the sum of solvent-solvent and solvent-solute interactions, coupled with the effect of the molecular weight of the components of the ILs or DESs formulations. In the context of DES and IL formulations, the pH of the formulation will undoubtedly play a contributing factor as it influences whether the predominant mechanism of interaction is mediated by dispersive interactions (i.e., hydrogen bonds or Van der Waals' interactions) or ion-ion interactions. Looking at Figure 2, the rheological behaviour of the formulations does not appear to follow a specific trend, with Ch-Trp exhibiting largely Newtonian flow, while ChCl-Urea displayed shear-thinning, pseudoplastic flow. Inversely, two of the three lowest viscosity formulations, BMPy, and Ch-Gly, despite some plate slippage, do both similarly appear to be largely Newtonian, while Ch-Pro exhibited shear-thinning, pseudoplastic flow. The lack of a trend in the rheological behaviour indicates the presence of a complex interaction; we postulate that specific intermolecular interactions are contributing to this behaviour; in Trp, the indole functional group allows for pi-pi interactions, coupled with the ionizability of the AA in the IL media, allows for stronger interactions resulting in greater viscosities, which is in agreement with previous reports on Ch-Trp viscosity [18]. Axiomatically, one may conclude that a simpler amino acid possessing a shorter carbon chain would exhibit lower viscosities; which was indeed observed with Ch-Gly, the shortest chain AA investigated, exhibiting the lowest overall viscosity. Inversely, longer-chain AAs (Val, Pro, and Lys) exhibited overall higher viscosities than shorter-chain AAs. This starkly different rheological behaviour of the tested formulations may largely be ascribed to the effect of molecular chain length and the nature of the intermolecular interaction in each formulation.
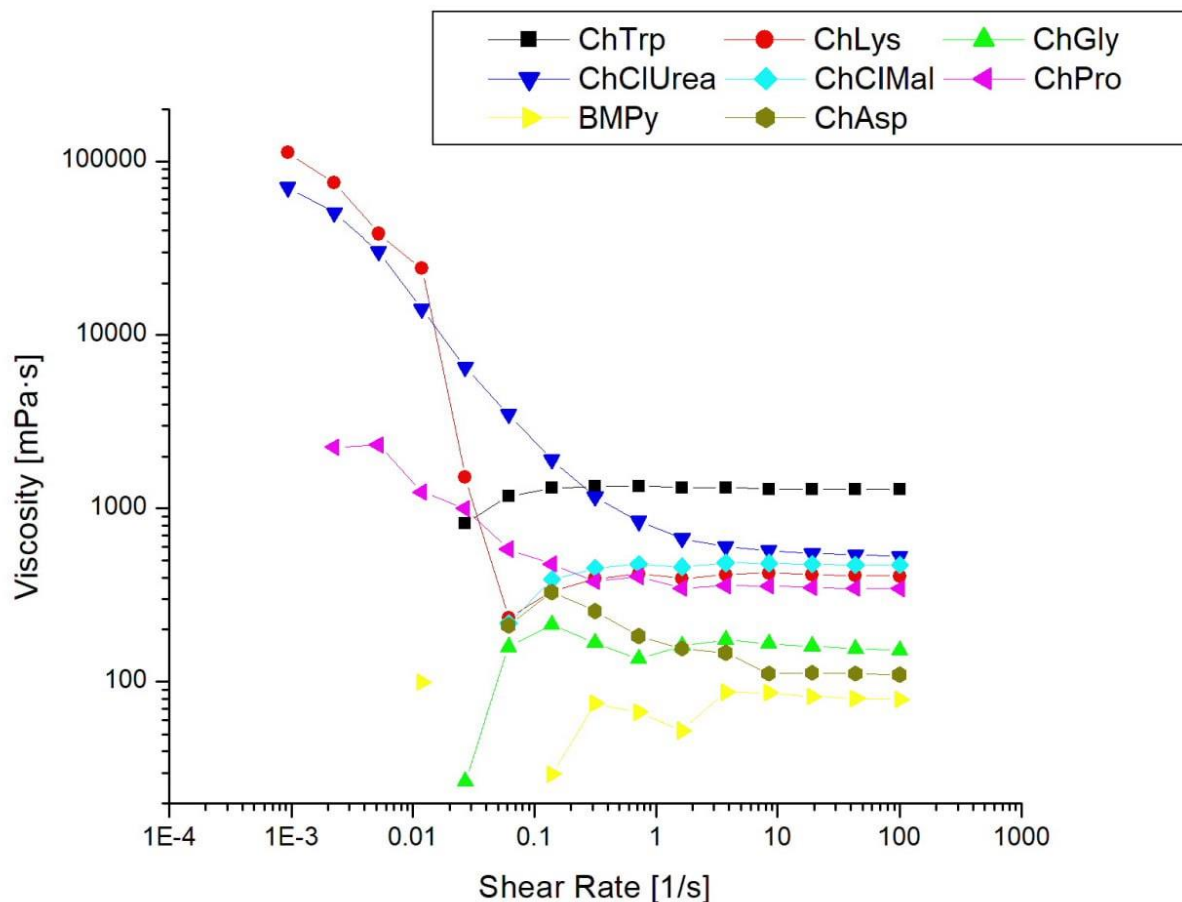
Figure 2. Rheological behaviours of the DESs and ILs prepared in this work.

Establishing stability studies with respect to thermal stress: Rational and design

The tendency to stabilise mAbs and maintain their structural and functional characteristics, particularly at high temperatures, offers several advantages, including facilitating the shipping and long-term storage processes and performing conjugation and enzymatic reactions [44,56]. Research has shown that elevated temperatures can cause protein aggregation with multiple domains, such as mAbs, by unfolding or partially unfolding the Fab and Fc domains. Denaturation of IgG occurs at high temperatures, resulting in irreversible aggregate formation and structural changes [34,57].

Atezolizumab (Amab) was selected as a model mAb to appraise the structural and functional impact of employing Ch-AA ILs as solvents or carriers. More importantly, Amab is an example of

an IgG1 antibody lacking the oligosaccharide attached to the Fc region produced by a N297A mutation. It is well-recognized that aglycosylation of IgG1 mAbs renders them unstable and more prone to aggregation [58]. Hence, we set out to provide a refined method to mitigate the aggregation potential of mAbs lacking the oligosaccharide moieties.

To holistically understand the impact of the prepared ILs and DESs on the stability of Amab, and the possibility of maintaining the structural and functional stability of Amab, samples were prepared in ILs or DESs and subjected to thermal stress conditions (RT, 45 and 55 °C). Characterisation of the higher order structure (HOS) and any form of degradation or aggregation was performed using UV-visible spectroscopy, DLS, SDS-PAGE and protein MS. For comparison purposes, Amab prepared in buffer (Tris.HCl, pH 7.4) without ILs or DESs, referred to as buffer sample was utilised and subjected to the various stress conditions. A fresh Amab sample, referred to as Amab control, was employed as a reference in SDS-PAGE, protein MS and MTT assay.

Following this, Amab formulations in AA ILs and DESS were prepared and found highly miscible with all the prepared AA ILs, and in ChCl-Urea. In contrast, protein precipitation was observed upon mixing Amab with ChCl-Mal and BMPy (Figure S9-12).

A- UV-Visible trace for Amab formulations in DESs

UV-visible spectroscopy allows one to infer any conformational changes of protein and the influence of ILs or DESs media on the tertiary structures of Amab as reflected by the change in λmax [59,60]. For comparison and understanding the changes in λmax, the spectrum of Amab control sample was initially measured and λmax was found at 280 nm as reported previously [58]. Protein solutions analyzed with UV spectrophotometry show a peak at 278-280 nm due to the response of aromatic residues of the amino acids phenylalanine, tyrosine and tryptophan to UV light. The shifting in λmax could reflect protein unfolding or aggregation due to exposing or changing the microenvironments of the aromatic amino acids [61]. For example, the shifting was used to study bovine serum albumin's degree of heat denaturation [62]. A hypsochromic shift was observed when surfactants were added to bovine serum albumin, reflecting the

binding of the surfactant to BSA, and changing the microenvironment around the aromatic amino acids [43].

In Figure 3A-C, the UV-visible spectroscopy showed that the λmax associated with the Amab remained unchanged at 280 nm after being incubated at RT for 1, 5 and 7 days and across the tested ChCl-Urea, Ch-Asp and Ch-Val formulations. According to the results, it could be concluded that there was a negligible impact on Amab's tertiary structure.

On the other hand, λmax shift was detected at RT incubation for 1 day with Ch-Pro (+10) and ChCl-Mal (-6) and to a lesser extent with BMPy (-4) and ChCl-Gly (+4), which could infer conformational changes and instability of Amab (Figure 3A-C).

Similarly, after the incubation at 45 °C and 55 °C, ChCl-Urea, Ch-Asp and Ch-Val exhibited no conformational changes of Amab, whereas BMPy exhibited a shift of the λmax (-5) (Figure 3D). The exact shift of each of the studied ILs and DESs and whether the shift was hypsochromic or bathochromic are illustrated in Table S1. It is worth mentioning that after exposure to thermal stress, Amab in Ch-Asp and BMPy exhibited hyperchromicity, reflecting more exposure to the aromatic AA and structural instability [63].

Next, in order to link the observed shift with the aggregation propensity, the aggregation index (AI) was calculated. It is widely known that reducing the antibody aggregates is essential in mitigating the risk immunogenicity of therapeutic mAbs [17]. Therefore, aggregation potential for the Amab samples at RT, 45 °C and 55 °C was calculated, and the determined AI is summarised in Table S1 and Table 2. AI below 10 is generally accepted for samples containing proteins representing solutions with no significant aggregation. Following this, no sufficient soluble aggregates were found across the samples prepared in DESs and ILs when kept for 24 hrs at RT, except BMPy, ChCl-Mal and Ch-Gly formulations (Table S2). However, Amab was incubated in ChCl-Urea, Ch-Aps or Ch-Val and subjected to 45 °C or 55 °C for 3 hrs, and a minimal increase in aggregation was observed. Contrary to BMPy formulation, a high AI was observed (Table 2).
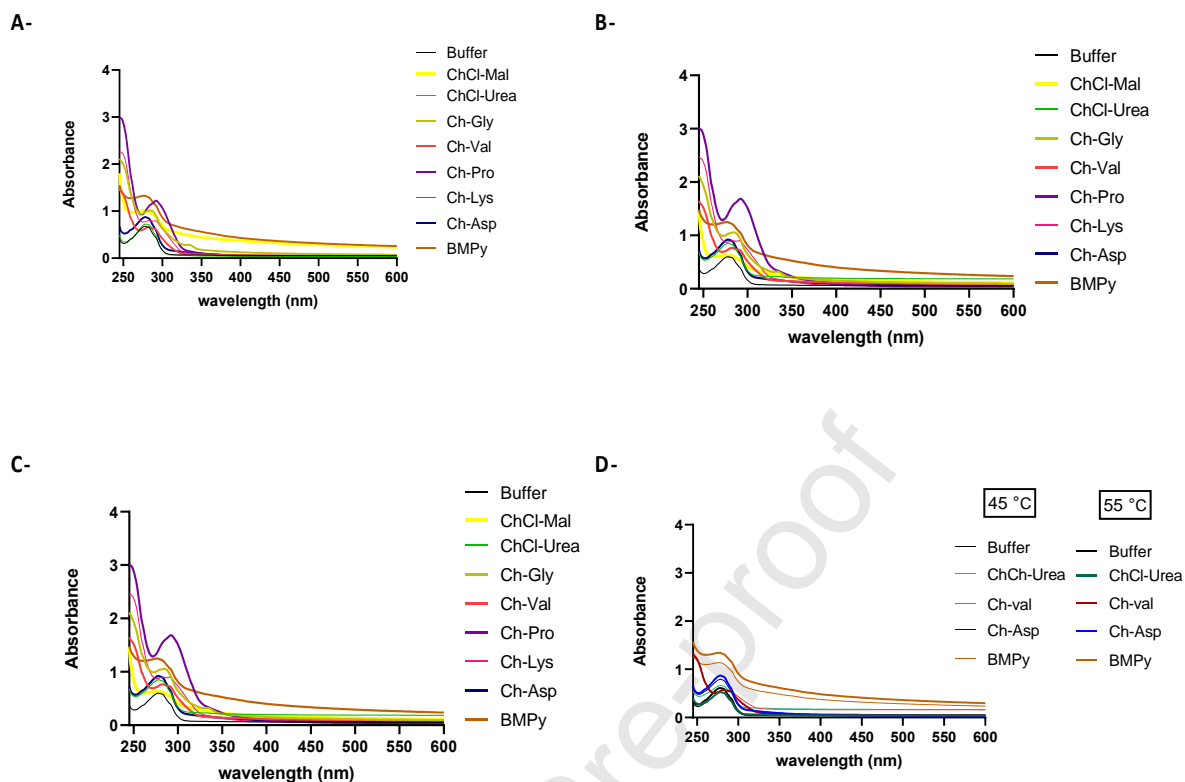
Figure 3. UV-visible absorbance spectra of Amab in the presence of various DESs and ILs. A- at RT after incubation for one day, B- for 5 days, C- for 7 days, and D- at 45 °C or 55 °C for 3hrs. Samples were measured directly as such without processing.

Table 2. Calculated AI for Amab samples.

	1 Day at RT	3 hrs at 45 °C	3 hrs at 55 °C
Buffer	7.31	7.26	10.00
ChCl-Urea	7.14	11.00	7.56
Ch-Val	15.09	17.81	19.47
Ch-Asp	15.00	14.00	15.35
BMPy	81.85	94.62	82.70

B- Measuring the hydrodynamic diameter measuring using DLS

To gain more understanding regarding the colloidal stability and aggregation propensity of Amab in the presence of DESs and ILs, the hydrodynamic diameter (D_r) was measured for Amab before and after incubation with the DESs and ILs at 3 temperature conditions (RT, 45 °C and 55 °C).

DLS is a commonly used technique to determine the average size of protein molecules or their aggregates in different solvents [57]. DLS results, D_r and polydispersity index (Pdi) are summarised in Table 3-5, Figure 4 and S13-19. In Buffer, the hydrodynamic diameter (D_r) of the Amab was centered around 10 nm. The buffer sample D_r agrees with monomeric IgG, as reported previously [57]. It was a relatively homogeneous size distribution, as it remains fairly consistent over the 10 days at RT, ranging from 10.06 to 10.99 nm. It also did not undergo any changes at the higher temperatures of 45 °C and 55 °C.
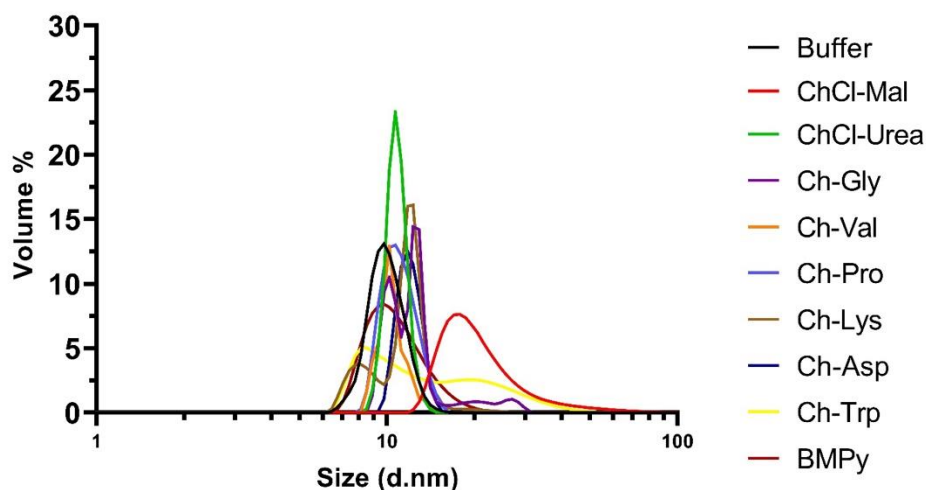

Figure 4. Amab particle size distribution was measured in the prepared ILs and DESs at zero time.

ChCl-Urea also has had a mild effect on the mAb's D_r at RT, suggesting that ChCl-Urea could potentially stabilise mAb without generating aggregates at RT. This could be attributed to ChCl-Urea pH (7.14), one of the closest tested liquids to a native protein pH environment. At 45°C, no noticeable changes were observed, while at 55 °C, the D_r increased by approximately three folds. This increase in D_r suggests the formation of aggregates due to the high temperature and that ChCl-Urea limit to prevent aggregates formation of mAb lies between 45 °C and 55 °C. Previously, ChCl-Urea was found promising in maintaining the structural stability of immunoglobulin G antibodies [36].

Glycine is a neutral amino acid with a small side chain. The increase in particle size in Ch-Gly over time and temperature suggests possible aggregation or structural changes. Amongst the

tested Ch-AA ILs, Ch-Val and Ch-Asp exhibited the most stable D_r across all tested temperatures. Valine is another neutral amino acid whose structure is similar to glycine but with a bulkier side chain. The relatively stable average hydrodynamic diameter values in Ch-Val across the tested temperatures suggest that valine has a limited effect on the mAb's particle size and distribution. This suggests that Ch-Val has the potential to stabilise mAb without any aggregate formation. These findings align with the overall results obtained in this study, confirming Ch-Val's ability to retain the colloidal stability of mAbs and possibly the biological activity under the studied high temperature conditions.

In Ch-Asp, D_r remained stable at all temperatures, suggesting some potential in Ch-Asp IL to provide sufficient stabilisation for mAb under different temperatures. Ch-Asp pH (6.1), being very close to optimum pH for protein function, may have played a role in its ability to stabilise Amab.

The substantial variations observed in the average hydrodynamic diameter in Ch-Pro, Ch-Lys and Ch-Trp ILs, indicate the formation of aggregates, which suggests an impact on the colloidal and structural stability of Amab and possibly a highly denatured state (Table 3-5). Lastly, BMPy and ChCl-Mal influence on D_r of Amab is apparent as significant changes can be observed over time and at different temperatures. It should be noted that neither liquid solubilised the mAb completely, which could be attributed to the observed increased hydrodynamic diameter (Figure S9-12, Table 3-5).

One can note that the Pdi values for many measurements were above 0.5, which reflects that the Amab solutions were polydisperse and colloidally unstable, particularly after being held at high temperatures. Similar observations were reported previously [36].

Table 3. Average hydrodynamic diameter with (Pdi) for the DESs and ILs, using five measurements, for 10 days at RT.

Media	Average hydrodynamic diameter and (Pdi)					
	Initial	1 Day	2 Days	5 Days	7 Days	10 Days
Buffer	10.01 (0.28)	10.35 (0.47)	10.59 (0.63)	10.55 (0.32)	10.99 (0.43)	10.06 (0.17)
ChCl-Mal	22.01 (0.68)	24.57 (0.35)	29.75 (1.0)	56.75 (1.0)	67.30 (0.37)	216.2 (0.84)
ChCl-Urea	10.80 (0.39)	10.06 (0.38)	10.67 (0.87)	10.20 (0.83)	9.67 (0.55)	9.10 (0.75)
Ch-Gly	11.26 (0.59)	22.66 (0.56)	39.76 (0.73)	40.50 (0.51)	25.60 (0.49)	29.50 (0.42)
Ch-Val	10.45 (0.21)	10.46 (0.72)	11.13 (0.73)	11.43 (0.52)	11.50 (0.52)	12.10 (0.51)
Ch-Pro	11.04 (0.635)	9.820 (0.41)	0.1100 (0.48)	144.0 (0.28)	323.0 (0.52)	344.0 (0.75)
Ch-Lys	11.43 (0.44)	10.94 (0.79)	1.320 (0.68)	35.00 (0.38)	64.30 (0.61)	258.2 (0.63)
Ch-Asp	11.95 (0.41)	10.29 (0.55)	11.16 (0.73)	10.21 (0.66)	10.15 (0.29)	197.6 (0.24)
Ch-Trp	15.91 (0.57)	25.86 (0.34)	35.19 (0.37)	59.00 (0.90)	31.20 (0.73)	1408 (0.36)
BMPy	10.90 (0.31)	11.25 (0.31)	31.74 (0.77)	167.2 (0.86)	45.70 (0.85)	33.10 (0.62)

Table 4. Average hydrodynamic diameter with (Pdi) for DESs and ILs, using five measurements, after incubation for 3 hrs at 45°C.

Media	Average hydrodynamic diameter and (Pdi)	
	Initial	After 3 hrs
Buffer	10.01 (0.28)	10.22 (0.47)
ChCl-Mal	22.01 (0.68)	426.0 (0.40)
ChCl-Urea	10.80 (0.39)	11.88 (0.52)
Ch-Gly	11.26 (0.59)	48.44 (0.58)
Ch-Val	10.45 (0.21)	10.40 (0.54)
Ch-Pro	11.04 (0.64)	34.65 (0.60)
Ch-Lys	11.43 (0.44)	9.040 (0.67)
Ch-Asp	11.95 (0.41)	11.48 (0.54)

Media	Average hydrodynamic diameter and (Pdi)	
	Initial	After 3 hrs
Ch-Trp	15.91 (0.57)	1,634 (0.74)
BMPy	10.90 (0.31)	11.22 (0.76)

Table 5. Average hydrodynamic diameter with Pdi for the ILs and DESs, using five measurements, after incubation for 3 hrs at 55°C.

Media	Average hydrodynamic diameter and (Pdi)	
	Initial	After 3 hrs
Buffer	10.01 (0.28)	10.27 (0.29)
Chcl-Mal	22.01 (0.68)	331.2 (0.53)
ChCl-Urea	10.80 (0.39)	29.91 (0.38)
Ch-Gly	11.26 (0.59)	1412 (0.57)
Ch-Val	10.45 (0.21)	10.65 (0.40)
Ch-Pro	11.04 (0.64)	0.8700 (0.75)
Ch-Lys	11.43 (0.44)	255.3 (0.58)
Ch-Asp	11.95 (0.41)	11.55 (0.43)
Ch-Trp	15.91 (0.57)	713.4 (0.79)
BMPy	10.90 (0.31)	790.6 (0.48)

C- SDS-PAGE characterisation of mAb

SDS-PAGE was performed to detect any degradation or aggregation and confirm structural integrity following the incubation of Amab with the ILs or DESs at 45 °C or 55 °C. Accordingly, the DESs and ILs formulations were compared with a fresh Amab sample, Amab control (Tris.HCl buffer, pH 7.4). Under reducing conditions, the control Amab showed two bands corresponding to the heavy chains (~50 kDa) and light chains (~25 kDa). Across the formulations, heavy chain and light chain were the main identified bands (Figure 5A, RD), confirming no significant structural changes (aggregation) or degradation of Amab. Generally, no signs of instability were observed except for Ch-Pro. ChCl-Urea and Ch-Asp gave two main bands with no sign of degradation or aggregation. On the other hand, higher molecular weight bands were observed with Ch-Gly, Ch-Val and Ch-Trp ILs, which could be protein aggregation (Figure 5A) [64].

The impact of the thermal stress was evaluated using reduced SDS-PAGE and gave similar behaviour (Figure S20A and B). It's worth mentioning that Amab samples incubated in ChCl-Mal gave inferior stability results compared to the other DESs and ILs, as confirmed by SDS-PAGE results (Figure S20C).

Having studied the impact of ILs and DESs under reducing conditions, we next set out to detect any possible aggregation at 45 °C or 55 °C incubation temperatures using SDS-PAGE resolved under non-reducing conditions. The optimum DESs and ILs, namely ChCl-Urea, Ch-Val and Ch-Asp, were resolved under non-reducing conditions and compared to the Amab buffer sample under similar conditions. To this end, SDS-PAGE elucidated that the aggregates formed with Ch-Val, as seen by reduced SDS-PAGE, were composed of noncovalently linked monomers as only one major band at about 150 kDa was observed for all formulations, similar to the control sample (NR) (Figure 5B).
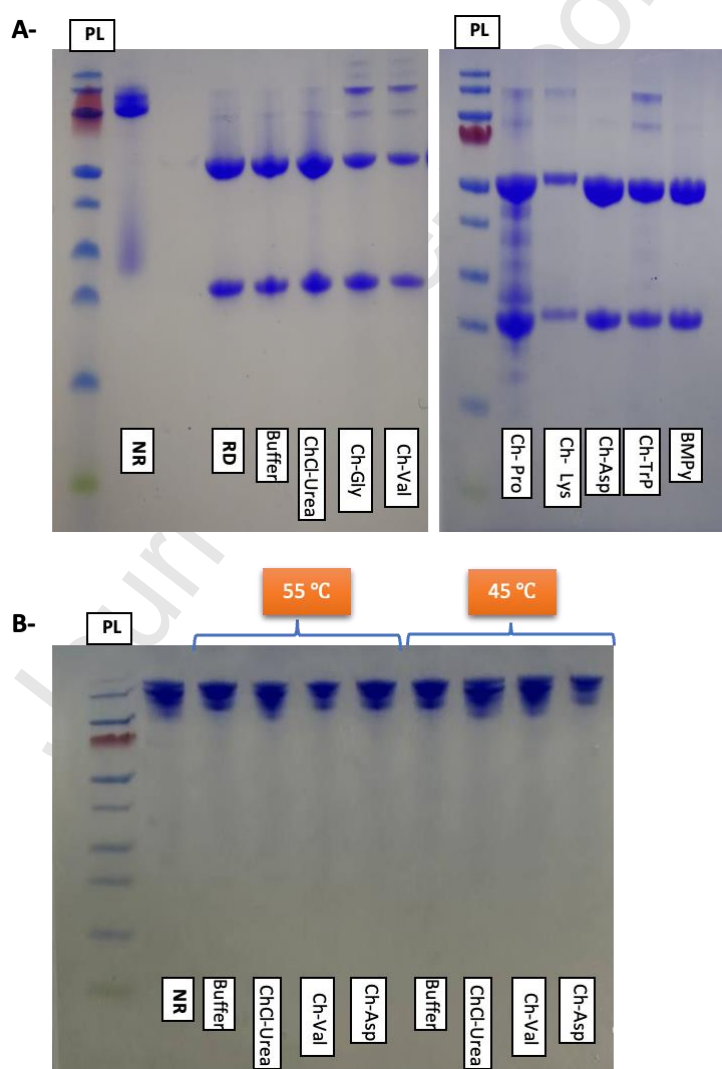

Figure 5. SDS-PAGE gel evaluating the stability of Amab formulations. A- At RT, PL: protein ladder. Amab control was run using a non-reducing dye (ND: None Reducing dye), and Amab control was run using a reducing dye (RD: Reducing dye). Protein samples were resolved by reducing conditions (10% gel).
B- At 45 °C and 55 °C, Protein samples were resolved under non-reducing conditions (10% gel).

D- Protein MS

Protein MS was performed to appraise any changes in the molecular weight of the heavy chain or the light chain of Amab after the incubation with the ILs or DESs. To this end, Amab incubated in buffer at RT for 24 hrs showed two prominent peaks at 23,361 Da and 48,824 Da of the light chain and heavy chain, respectively (Figure 6). The formulations were compared with Amab control (Figure S21A). Amab incubated ILs, namely, Ch-Gly, Ch-Lys, Ch-Trp and BMPy, exhibited small molecular weight peaks of less than 20,000 Da, which could be degradation peaks. Amab incubated in Ch-Asp showed a spectrum similar to that of the buffer with no sign of degradation (Figure 6).

Optimum formulations, namely, ChCl-Urea, Ch-Gly, Ch-Val and Ch-Asp, were incubated at 45 °C and 55 °C for 3 hrs. All the samples showed degradation peaks below 20,000 Da, along with the buffer sample (Figure 7).

It is worthwhile to mention that the ChCh-Mal formulation gave peaks at 90,000 Da (under reducing conditions), which could be a form of aggregation (Figure S21B).
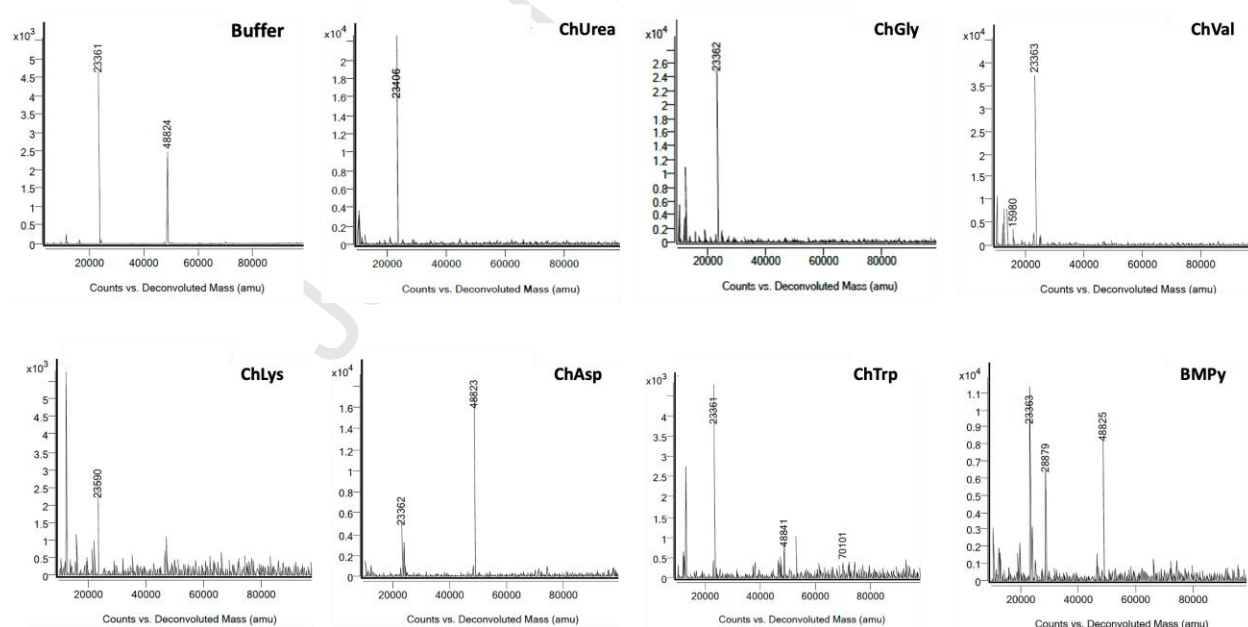

Figure 6. Deconvoluted MS results of Amab formulations after storage for 24 hrs at RT.
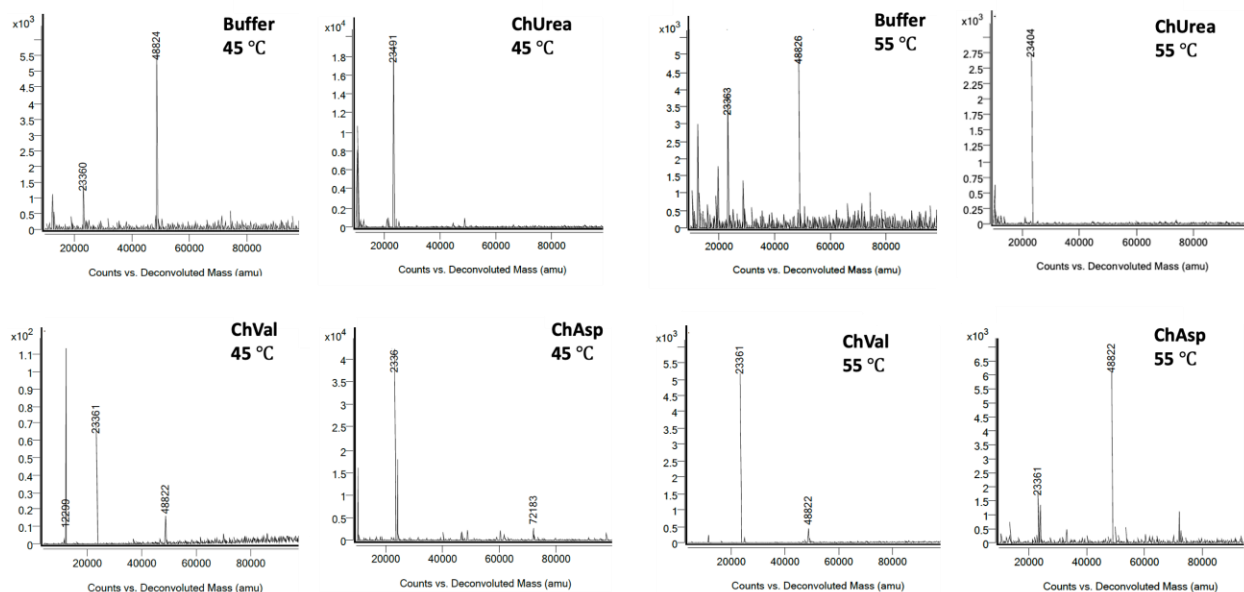
Figure 7. Deconvoluted MS data of Amab formulations after storage for 3hrs at 45 °C or 55 °C.

Overall, the stability results of the Amab in the tested Ch-AA ILs formulations were found to have superior structural stability of Amab when compared with the ChCl-Mal, BMPy formulations, particularly at 55 °C. This could be partly attributed to the optimum pH or/and low viscosity (Table 1). The low pH of both ChCl-Mal (1.95) and BMPy (4.47) liquids could be the main factor attributed to their observed instability. It's well-known that low pH triggers the unfolding, denaturation, and aggregation of mAbs, and previous studies have demonstrated the main impact of extremely low pH on the stability of the Fc region of mAbs [33,65]. It has been reported that BMPy could be used in bioconjugation reactions to modify mAbs and proteins at 50 °C. Nevertheless, our findings have demonstrated that BMPy was inferior to the AA-based ILs in maintaining the structural stability of Amab, particularly at 55 °C. For Table 1, one can note that the Ch-Val process has a relatively intermediate viscosity compared to the other ILs and DESs. Therefore, the optimum viscosity of Ch-Val marginally attributes to the higher stability and the lower tendency of aggregation.

To the best of our knowledge, this work describes for the first time the different impacts of functional groups of Ch-AA ILs and how they are linked to their implications. Generally, AA-based are highly viscous solvents, with polar AA being more viscous. Valine belongs to non-

polar AA with a small hydrophobic functional group, suggesting that this group (non-polar AAs) is superior in enhancing the stability of mAbs.

The non-toxic and renewable class of AA-based ILs provided in this work, particularly Ch-Val, was found optimum in maintaining the structural stability of Amab under the studied conditions as conformed by the Uv-Visible trace of Amab and Protein MS. In addition, as illustrated by DLS results, only the buffer and Ch-Val formulations showed peaks close to (10 nm) in D_r, indicating their ability to protect mAb from unfolding or forming aggregates after ten days of storage at RT. Other AA-ILs could not stabilise Amab efficiently compared to buffer, except for Ch-Asp, as it showed peaks at (10 nm) D_r after one week of storage at RT and exhibited a lower trend of degradation or aggregation peaks in SDS-PAGE and protein MS studies.

In vitro activity of Amab using MTT assay

To elucidate their superiority in maintaining biocompatibility and functionality, the optimum Ch-AA formulations of Amab, Ch-Val, and Ch-Asp and ChCl-Urea were incubated at 55 °C for 3 hrs, and the biological activity of Amab was evaluated using MTT assay. All the formations were compared with Amab control (a fresh Amab sample in Tris.HCl buffer, pH 7.4) (Figure 8A). Initially, the optimum time for the assay was determined, and according to the attained results, 48 hrs of incubation with Amab were sufficient to reduce cell viability to almost 50% at 200 μg/ml (Figure 8A). The assay was challenged with 25% DMSO as a positive control. Thus, the results showed a significant reduction in cell viability compared to negative control (untreated cells) with a *p*-value ≤ 0.0001.

Having established the optimum incubation conditions, the optimum Amab formulations were subjected to 55 °C for 3 hrs and their antitumor activity against EMT6 cells was evaluated. To this end, Figure 8B shows that the buffer sample and all the tested formulations of Amab exhibited a significant increase in cell viability, reflecting the deteriorated activity of Amab. Nevertheless, amongst the tested formulations, Ch-Val IL was found optimal in retaining the activity of Amab (cell viability was 77.27%).
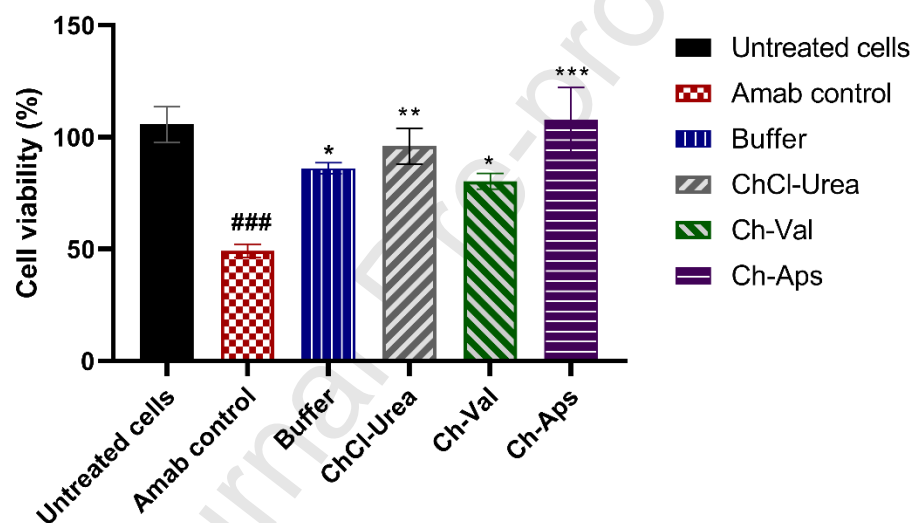
A-
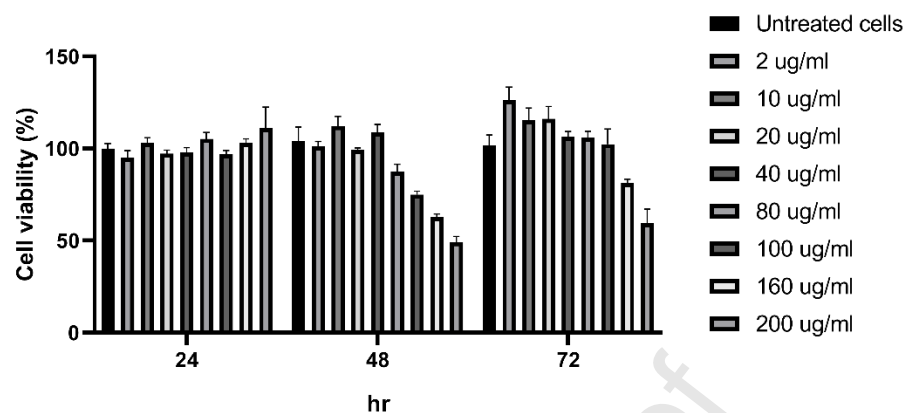
B-

Figure 8. Cytotoxicity assay (MTT) results using EMT6 cells. A- EMT6 cells were incubated with Amab control for different time intervals. B- EMT6 cells were incubated with Amab formulations for 48 hrs. *, **, ***: Statistical difference in comparison to Amab control with a p-values <0.05, <0.01, <0.001, respectively. ### statistical difference in comparison with untreated cells p-value <0.001. The data represent the mean + SD (n=4). Amab control (a fresh Amab sample in Tris.HCl, pH 7.4). Amab prepared in buffer (Tris.HCl, pH 7.4) without ILs or DESs, referred to as buffer sample, was subjected to similar stress conditions.

Conclusion

In conclusion, the reports in this area focused on enzymes and how to use DESs and ILs to stabilise them. Herein, this is one of the few reports centred on expanding the utility of green and bio-based ILs in the field of mAbs, the fastest-growing class of biologics.

The non-toxic and renewable class of AA-based ILs provided in this work, particularly Ch-Val, were superior in maintaining the structural and functional stability of Amab, particularly at 55

26

ºC. The results support exploiting the advantages of AA-based ILs in mAbs formulations, particularly the non-polar class of AAs, for packaging, long-term storage, and many other uses. Future work could elucidate the mechanisms behind the observed functional and structural stabilising.

Conflicts of interest

The authors declare that they have no known competing financial interests or personal relationships that could have appeared to influence the work reported in this paper.

Acknowledgements

Author contributions

BA: Conceptualization, Methodology, Investigation, Data Curation, Resources, Visualization, Writing - Original Draft. **FA**: Resources, Supervision, Writing - Review & Editing, Methodology. **ZA:** Methodology, Investigation, Writing - Review & Editing, Data Curation. **GA**: Investigation, Methodology, Validation. **MB**: Investigation, Writing - Review & Editing, Methodology. **MS**: Formal analysis, Investigation, Methodology. **ASAAA**: Formal analysis, Investigation, Methodology. **JN**: Formal analysis, Methodology, Writing - Review & Editing. **NQ**: Resources, Methodology. **AM**: Methodology, Writing - Review & Editing. **AGW:** Resources, Supervision.

References

[1]   B.B. Hansen, S. Spittle, B. Chen, D. Poe, Y. Zhang, J.M. Klein, A. Horton, L. Adhikari, T. Zelovich, B.W. Doherty, B. Gurkan, E.J. Maginn, A. Ragauskas, M. Dadmun, T.A. Zawodzinski, G.A. Baker, M.E. Tuckerman, R.F. Savinell, J.R. Sangoro, Deep Eutectic Solvents: A Review of Fundamentals and Applications, Chem. Rev. 121 (2021) 1232–1285. https://doi.org/10.1021/ACS.CHEMREV.0C00385/ASSET/IMAGES/MEDIUM/CR0C00385_0009.GIF.

[2]   R. Hayes, G.G. Warr, R. Atkin, Structure and Nanostructure in Ionic Liquids, Chem. Rev. 115 (2015) 6357–6426. https://doi.org/10.1021/CR500411Q/ASSET/IMAGES/LARGE/CR-2014-00411Q_0035.JPEG.

[3]   M. Uddin, D. Basak, R. Hopefl, B. Minofar, Potential Application of Ionic Liquids in Pharmaceutical Dosage Forms for Small Molecule Drug and Vaccine Delivery System, J. Pharm. Pharm. Sci. 23 (2020) 158–176. https://doi.org/10.18433/JPPS30965.

[4]   R. Md Moshikur, M.R. Chowdhury, M. Moniruzzaman, M. Goto, Biocompatible ionic liquids and their applications in pharmaceutics, Green Chem. 22 (2020) 8116–8139. https://doi.org/10.1039/d0gc02387f.

[5]   T. Hattori, H. Tagawa, M. Inai, T. Kan, S. ichiro Kimura, S. Itai, S. Mitragotri, Y. Iwao, Transdermal delivery of nobiletin using ionic liquids, Sci. Reports 2019 91. 9 (2019) 1–11. https://doi.org/10.1038/s41598-019-56731-1.

[6]   F. Al-Akayleh, S. Adwan, M. Khanfer, N. Idkaidek, M. Al-Remawi, A Novel Eutectic-Based Transdermal Delivery System for Risperidone, AAPS PharmSciTech. 22 (2020). https://doi.org/10.1208/S12249-020-01844-4.

[7]   P. Lozano, J.M. Bernal, E. Garcia-Verdugo, G. Sanchez-Gomez, M. Vaultier, M.I. Burguete, S. V. Luis, Sponge-like ionic liquids: a new platform for green biocatalytic chemical processes, Green Chem. 17 (2015) 3706–3717. https://doi.org/10.1039/C5GC00894H.

[8]   M. Guncheva, K. Paunova, D. Yancheva, I. Svinyarov, M. Bogdanov, Effect of two series ionic liquids based on non-nutritive sweeteners on catalytic activity and stability of the industrially important lipases from Candida rugosa and Rhizopus delemar, J. Mol. Catal. B Enzym. 117 (2015) 62–68. https://doi.org/10.1016/J.MOLCATB.2015.04.009.

[9]   F.D.' Anna, A. Mulchandani, L. Campanella, A.K. Croft, A. Schindl, M.L. Hagen, S. Muzammal, H.A.D. Gunasekera, Proteins in Ionic Liquids: Reactions, Applications, and Futures, Front. Chem. | Www.Frontiersin.Org. 1 (2019) 347. https://doi.org/10.3389/fchem.2019.00347.

[10]   P. Angsantikul, K. Peng, A.M. Curreri, Y. Chua, K.Z. Chen, J. Ehondor, S. Mitragotri, Ionic Liquids and Deep Eutectic Solvents for Enhanced Delivery of Antibodies in the Gastrointestinal Tract, Adv. Funct. Mater. 31 (2021) 2002912. https://doi.org/10.1002/ADFM.202002912.

[11]   A. Banerjee, K. Ibsen, T. Brown, R. Chen, C. Agatemor, S. Mitragotri, Ionic liquids for oral insulin delivery, Proc. Natl. Acad. Sci. U. S. A. 115 (2018) 7296–7301. https://doi.org/10.1073/PNAS.1722338115/SUPPL_FILE/PNAS.1722338115.SAPP.PDF.

[12]   A.A.M. Elgharbawy, M. Moniruzzaman, M. Goto, Recent advances of enzymatic reactions in ionic liquids: Part II, Biochem. Eng. J. 154 (2020). https://doi.org/10.1016/J.BEJ.2019.107426.

[13]   P. Attri, P. Venkatesu, A. Kumar, Activity and stability of α-chymotrypsin in biocompatible ionic liquids: enzyme refolding by triethyl ammonium acetate, Phys. Chem. Chem. Phys. 13 (2011) 2788–2796. https://doi.org/10.1039/C0CP01291B.

[14]   M. Bisht, D. Mondal, M.M. Pereira, M.G. Freire, P. Venkatesu, J.A.P. Coutinho, Long-term protein packaging in cholinium-based ionic liquids: improved catalytic activity and

enhanced stability of cytochrome c against multiple stresses, Green Chem. 19 (2017) 4900–4911. https://doi.org/10.1039/C7GC02011B.

[15]   D. Mondal, M. Sharma, M. V. Quental, A.P.M. Tavares, K. Prasad, M.G. Freire, Suitability of bio-based ionic liquids for the extraction and purification of IgG antibodies, Green Chem. 18 (2016) 6071–6081. https://doi.org/10.1039/C6GC01482H.

[16]   H.M. El-Shaffey, E.J. Gross, Y.D. Hall, J. Ohata, An Ionic Liquid Medium Enables Development of a Phosphine-Mediated Amine-Azide Bioconjugation Method, J. Am. Chem. Soc. 143 (2021) 12974–12979. https://doi.org/10.1021/JACS.1C06092/SUPPL_FILE/JA1C06092_SI_001.PDF.

[17]   M. Reslan, V. Ranganathan, D.R. Macfarlane, V. Kayser, Choline ionic liquid enhances the stability of Herceptin® (trastuzumab), Chem. Commun. 54 (2018) 10622–10625. https://doi.org/10.1039/C8CC06397D.

[18]   Q.P. Liu, X.D. Hou, N. Li, M.H. Zong, Ionic liquids from renewable biomaterials: synthesis, characterization and application in the pretreatment of biomass, Green Chem. 14 (2012) 304–307. https://doi.org/10.1039/C2GC16128A.

[19]   W. Deng, L. Liu, Y. Peng, Choline taurinate: A new biocompatible amino-functionalized ionic liquid as basic catalyst and extraction solvent, Green Process. Synth. 7 (2018) 191–197. https://doi.org/10.1515/GPS-2017-0009/DOWNLOADASSET/SUPPL/GPS-2017-0009_SUPPL.DOC.

[20]   S. Miao, R. Atkin, G. Warr, Design and applications of biocompatible choline amino acid ionic liquids, Green Chem. 24 (2022) 7281–7304. https://doi.org/10.1039/D2GC02282F.

[21]   M. Guncheva, P. Ossowicz, E. Janus, S. Todinova, D. Yancheva, Elucidation of the effect of some cholinium amino acid ionic liquids on the thermal and the conformational stability of insulin, J. Mol. Liq. 283 (2019) 257–262. https://doi.org/10.1016/J.MOLLIQ.2019.03.074.

[22]   D.K. Sahoo, S. Jena, K.D. Tulsiyan, J. Dutta, S. Chakrabarty, H.S. Biswal, Amino-Acid-Based Ionic Liquids for the Improvement in Stability and Activity of Cytochrome c: A Combined Experimental and Molecular Dynamics Study, J. Phys. Chem. B. 123 (2019) 10100–10109. https://doi.org/10.1021/ACS.JPCB.9B09278.

[23]   D. Zahavi, L. Weiner, Monoclonal Antibodies in Cancer Therapy, Antibodies 2020, Vol. 9, Page 34. 9 (2020) 34. https://doi.org/10.3390/ANTIB9030034.

[24]   H. Kaplon, A. Chenoweth, S. Crescioli, J.M. Reichert, Antibodies to watch in 2022, MAbs. 14 (2022). https://doi.org/10.1080/19420862.2021.2014296.

[25]   L.M. Weiner, R. Surana, S. Wang, Monoclonal antibodies: versatile platforms for cancer immunotherapy, Nat. Rev. Immunol. 10 (2010) 317–327. https://doi.org/10.1038/NRI2744.

[26]   C. Robert, A decade of immune-checkpoint inhibitors in cancer therapy, Nat. Commun.

2020 111. 11 (2020) 1–3. https://doi.org/10.1038/s41467-020-17670-y.

[27] P. Darvin, S.M. Toor, V. Sasidharan Nair, E. Elkord, Immune checkpoint inhibitors: recent progress and potential biomarkers, Exp. Mol. Med. 50 (2018) 165. https://doi.org/10.1038/s12276-018-0191-1.

[28] K.M. Hargadon, C.E. Johnson, C.J. Williams, Immune checkpoint blockade therapy for cancer: An overview of FDA-approved immune checkpoint inhibitors, Int. Immunopharmacol. 62 (2018) 29–39. https://doi.org/10.1016/J.INTIMP.2018.06.001.

[29] M. de Miguel, E. Calvo, Clinical Challenges of Immune Checkpoint Inhibitors, Cancer Cell. 38 (2020) 326–333. https://doi.org/10.1016/J.CCELL.2020.07.004.

[30] Q. Lei, D. Wang, K. Sun, L. Wang, Y. Zhang, Resistance Mechanisms of Anti-PD1/PDL1 Therapy in Solid Tumors, Front. Cell Dev. Biol. 8 (2020) 672. https://doi.org/10.3389/FCELL.2020.00672/BIBTEX.

[31] R.M. Lu, Y.C. Hwang, I.J. Liu, C.C. Lee, H.Z. Tsai, H.J. Li, H.C. Wu, Development of therapeutic antibodies for the treatment of diseases, J. Biomed. Sci. 2020 271. 27 (2020) 1–30. https://doi.org/10.1186/S12929-019-0592-Z.

[32] N.B. Pham, W.S. Meng, Protein Aggregation and Immunogenicity of Biotherapeutics, Int. J. Pharm. 585 (2020) 119523. https://doi.org/10.1016/J.IJPHARM.2020.119523.

[33] H. Kaur, Stability testing in monoclonal antibodies, Crit. Rev. Biotechnol. 41 (2021) 692–714. https://doi.org/10.1080/07388551.2021.1874281.

[34] A.W.P. Vermeer, W. Norde, The thermal stability of immunoglobulin: unfolding and aggregation of a multi-domain protein., Biophys. J. 78 (2000) 394. https://doi.org/10.1016/S0006-3495(00)76602-1.

[35] S.N. Pedro, M.G. Freire, C.S.R. Freire, A.J.D. Silvestre, Deep eutectic solvents comprising active pharmaceutical ingredients in the development of drug delivery systems, Https://Doi.Org/10.1080/17425247.2019.1604680. 16 (2019) 497–506. https://doi.org/10.1080/17425247.2019.1604680.

[36] D. Dhiman, A.S.C. Marques, M. Bisht, A.P.M. Tavares, M.G. Freire, P. Venkatesu, Unveiling the potential of deep eutectic solvents to improve the conformational and colloidal stability of immunoglobulin G antibodies, Green Chem. 25 (2023) 650–660. https://doi.org/10.1039/D2GC03415H.

[37] T.A. Shmool, L.K. Martin, R.P. Matthews, J.P. Hallett, Ionic Liquid-Based Strategy for Predicting Protein Aggregation Propensity and Thermodynamic Stability, JACS Au. 2 (2022) 2068–2080. https://doi.org/10.1021/JACSAU.2C00356/ASSET/IMAGES/MEDIUM/AU2C00356_M006. GIF.

[38] T.A. Shmool, L.K. Martin, L. Bui-Le, I. Moya-Ramirez, P. Kotidis, R.P. Matthews, G.A. Venter, C. Kontoravdi, K.M. Polizzi, J.P. Hallett, An experimental approach probing the

conformational transitions and energy landscape of antibodies: a glimmer of hope for reviving lost therapeutic candidates using ionic liquid, Chem. Sci. 12 (2021) 9528–9545. https://doi.org/10.1039/D1SC02520A.

[39]   B. Alkhawaja, F. Al-Akayleh, A. Al-Khateeb, J. Nasereddin, B.Y. Ghanim, A. Bolhuis, N. Jaber, M. Al-Remawi, N.A. Qinna, Deep Eutectic Liquids as a Topical Vehicle for Tadalafil: Characterisation and Potential Wound Healing and Antimicrobial Activity, Molecules. 28 (2023) 2402. https://doi.org/10.3390/MOLECULES28052402/S1.

[40]   C. Teja, F.R. Nawaz Khan, Choline Chloride-Based Deep Eutectic Systems in Sequential Friedländer Reaction and Palladium-Catalyzed sp 3 CH Functionalization of Methyl Ketones, ACS Omega. 4 (2019) 8046–8055. https://doi.org/10.1021/ACSOMEGA.9B00310/ASSET/IMAGES/LARGE/AO-2019-00310A_0007.JPEG.

[41]   N. Azizi, S. Dezfooli, M.M. Hashemi, A sustainable approach to the Ugi reaction in deep eutectic solvent, Comptes Rendus Chim. 16 (2013) 1098–1102. https://doi.org/10.1016/J.CRCI.2013.05.013.

[42]   G. Latini, M. Signorile, V. Crocellà, S. Bocchini, C.F. Pirri, S. Bordiga, Unraveling the CO_2 reaction mechanism in bio-based amino-acid ionic liquids by operando ATR-IR spectroscopy, Catal. Today. 336 (2019) 148–160. https://doi.org/10.1016/j.cattod.2018.12.050.

[43]   A. Sharma, P.K. Agarwal, S. Deep, Characterization of different conformations of bovine serum albumin and their propensity to aggregate in the presence of N-cetyl-N,N,N-trimethyl ammonium bromide, J. Colloid Interface Sci. 343 (2010) 454–462. https://doi.org/10.1016/J.JCIS.2009.12.012.

[44]   A.P.S. Brogan, J.P. Hallett, Solubilizing and Stabilizing Proteins in Anhydrous Ionic Liquids through Formation of Protein-Polymer Surfactant Nanoconstructs, J. Am. Chem. Soc. 138 (2016) 4494–4501. https://doi.org/10.1021/JACS.5B13425/ASSET/IMAGES/LARGE/JA-2015-134259_0004.JPEG.

[45]   S. De Santis, G. Masci, F. Casciotta, R. Caminiti, E. Scarpellini, M. Campetella, L. Gontrani, Cholinium-amino acid based ionic liquids: a new method of synthesis and physico-chemical characterization, Phys. Chem. Chem. Phys. 17 (2015) 20687–20698. https://doi.org/10.1039/C5CP01612F.

[46]   Q.P. Liu, X.D. Hou, N. Li, M.H. Zong, Ionic liquids from renewable biomaterials: synthesis, characterization and application in the pretreatment of biomass, Green Chem. 14 (2012) 304–307. https://doi.org/10.1039/C2GC16128A.

[47]   A. Rawat, S.S. Gupta, H. Kalluri, M. Lowenborg, K. Bhatia, K. Warner, Rheological Characterization in the Development of Topical Drug Products, AAPS Adv. Pharm. Sci. Ser. 36 (2019) 3–45. https://doi.org/10.1007/978-3-030-17355-5_1/FIGURES/31.

[48]   T. Peppel, M. Köckerling, M. Geppert-Rybczyńska, R. V. Ralys, J.K. Lehmann, S.P.

Verevkin, A. Heintz, Low-Viscosity Paramagnetic Ionic Liquids with Doubly Charged [Co(NCS)4]2− Ions, Angew. Chemie Int. Ed. 49 (2010) 7116–7119. https://doi.org/10.1002/ANIE.201000709.

[49]   C.H. Schein, Solubility as a Function of Protein Structure and Solvent Components, Nat. Biotechnol. 8 (1990) 308–317. https://doi.org/10.1038/nbt0490-308.

[50]   M. Sleutel, A.E.S. Van Driessche, W. Pan, E.K. Reichel, D. Maes, P.G. Vekilov, Does solution viscosity scale the rate of aggregation of folded proteins?, J. Phys. Chem. Lett. 3 (2012) 1258–1263. https://doi.org/10.1021/JZ300459N/SUPPL_FILE/JZ300459N_SI_004.AVI.

[51]   Y. Yu, X. Lu, Q. Zhou, K. Dong, H. Yao, S. Zhang, Biodegradable naphthenic acid ionic liquids: synthesis, characterization, and quantitative structure-biodegradation relationship, Chemistry. 14 (2008) 11174–11182. https://doi.org/10.1002/CHEM.200800620.

[52]   J.J. Hung, B.J. Dear, A.K. Dinin, A.U. Borwankar, S.K. Mehta, T.T. Truskett, K.P. Johnston, Improving Viscosity and Stability of a Highly Concentrated Monoclonal Antibody Solution with Concentrated Proline, Pharm. Res. 35 (2018). https://doi.org/10.1007/S11095-018-2398-1.

[53]   L. Zandarashvili, D.W. Li, T. Wang, R. Brüschweiler, J. Iwahara, Signature of mobile hydrogen bonding of lysine side chains from long-range 15N-13C scalar J-couplings and computation, J. Am. Chem. Soc. 133 (2011) 9192–9195. https://doi.org/10.1021/JA202219N/SUPPL_FILE/JA202219N_SI_001.PDF.

[54]   G. Gygli, X. Xu, J. Pleiss, Meta-analysis of viscosity of aqueous deep eutectic solvents and their components, Sci. Reports 2020 101. 10 (2020) 1–11. https://doi.org/10.1038/s41598-020-78101-y.

[55]   Y.P. Hsieh, R.B. Leron, A.N. Soriano, A.R. Caparanga, M.H. Li, Diusivity, density and viscosity of aqueous solutions of choline chloride/ethylene glycol and choline chloride/malonic acid, J. Chem. Eng. Japan. 45 (2012) 939–947. https://doi.org/10.1252/JCEJ.12WE128.

[56]   W. Wang, S. Singh, D.L. Zeng, K. King, S. Nema, Antibody structure, instability, and formulation, J. Pharm. Sci. 96 (2007) 1–26. https://doi.org/10.1002/JPS.20727.

[57]   A. Hawe, J.C. Kasper, W. Friess, W. Jiskoot, Structural properties of monoclonal antibody aggregates induced by freeze-thawing and thermal stress, Eur. J. Pharm. Sci. 38 (2009) 79–87. https://doi.org/10.1016/J.EJPS.2009.06.001.

[58]   M. Li, R. Zhao, J. Chen, W. Tian, C. Xia, X. Liu, Y. Li, S. Li, H. Sun, T. Shen, W. Ren, L. Sun, Next generation of anti-PD-L1 Atezolizumab with enhanced anti-tumor efficacy in vivo, Sci. Reports 2021 111. 11 (2021) 1–11. https://doi.org/10.1038/s41598-021-85329-9.

[59]   L. Bui-Le, C.J. Clarke, A. Bröhl, A.P.S. Brogan, J.A.J. Arpino, K.M. Polizzi, J.P. Hallett, Revealing the complexity of ionic liquid–protein interactions through a multi-technique

investigation, Commun. Chem. 2020 31. 3 (2020) 1–9. https://doi.org/10.1038/s42004-020-0302-5.

[60] D. Dhiman, S. Mor, U. Fatima, P. Venkatesu, Impact of ZIF-8, ArgHCl, and Ionic Liquid-Based Formulations on the Conformational and Colloidal Stability of Antibodies, Mol. Pharm. 20 (2023) 3150–3159. https://doi.org/10.1021/ACS.MOLPHARMACEUT.3C00167/SUPPL_FILE/MP3C00167_SI_001.PDF.

[61] F. Schmid, Biological Macromolecules: UV-visible Spectrophotometry, ELS. (2001) 1–4. https://doi.org/10.1038/npg.els.0003142.

[62] A. Nikolaidis, T. Moschakis, Studying the denaturation of bovine serum albumin by a novel approach of difference-UV analysis, Food Chem. 215 (2017) 235–244. https://doi.org/10.1016/J.FOODCHEM.2016.07.133.

[63] S. Islam, Moinuddin, A.R. Mir, M.Y. Arfat, K. Alam, A. Ali, Studies on glycoxidatively modified human IgG: Implications in immuno-pathology of type 2 diabetes mellitus, Int. J. Biol. Macromol. 104 (2017) 19–29. https://doi.org/10.1016/J.IJBIOMAC.2017.05.190.

[64] D. Dhiman, M. Bisht, A.P.M. Tavares, M.G. Freire, P. Venkatesu, Cholinium-Based Ionic Liquids as Efficient Media for Improving the Structural and Thermal Stability of Immunoglobulin G Antibodies, ACS Sustain. Chem. Eng. 10 (2022) 5404–5420. https://doi.org/10.1021/ACSSUSCHEMENG.1C07979/SUPPL_FILE/SC1C07979_SI_001.PDF.

[65] A.W.P. Vermeer, W. Norde, The thermal stability of immunoglobulin: unfolding and aggregation of a multi-domain protein, Biophys. J. 78 (2000) 394–404. https://doi.org/10.1016/S0006-3495(00)76602-1.
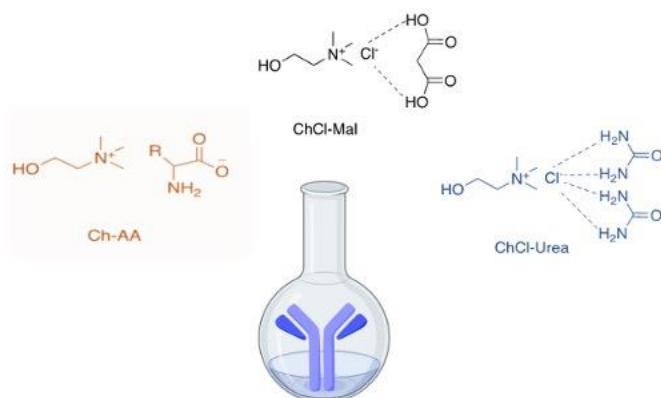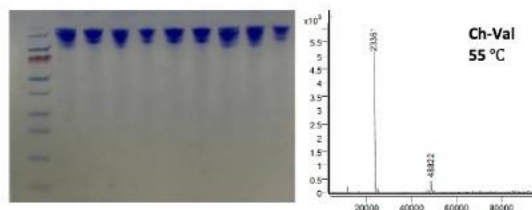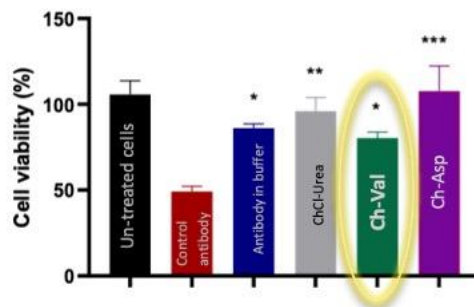
Graphical abstract

Highlights

❖ A series of AA-based ILs and Choline-based DESs were utilised to stabilise mAbs

❖ Colloidal stability of Amab in the ILs and DESs was studied using various techniques

❖ The advantages of adopting Valine-based IL in therapeutic mAbs formulations were revealed

❖ AA-based ILs demonstrated superior effectiveness in maintaining the biological activity of mAbs